RSC Advances

PAPER

View Article Online
View Journal | View Issue



Cite this: *RSC Adv.*, 2023, **13**, 21414

# Simple and sensitive detection of miRNA-122 based on a micro-biosensor through square wave voltammetry

Jiali Zhai,†[a] Huiyuan Sun,†[b] Mingkang Li,[c] Yuhao Gao,[c] Yixin Hu,[c] Zhi Gao,[d] Xiyu Xie,[d] Lixia Zhang*[e] and Guangtao Zhao *[e]

The simple and sensitive detection of miRNA-122 in blood is crucially important for early hepatocellular carcinoma (HCC) diagnosis. In this work, a platinum microelectrode (PtμE) was prepared and electrodeposited with molybdenum disulfide ($MoS_2$) and gold nanoparticles (AuNP), respectively, and denoted as PtμE/$MoS_2$/Au. The prepared PtμE/$MoS_2$/Au was used as the microsensor for the detection of miRNA-122 combined with the probe DNA as a biorecognition element which is the complementary strand of miRNA-122. The PtμE/$MoS_2$/Au conjugated with the probe DNA modified with sulfydryl units was used as the micro-biosensor for the detection of miRNA-122. The square wave voltammetry was performed for the quantitative detection of miRNA-122 using $[Fe(CN)_6]^{4-/3-}$ as a mediator. Under the optimized conditions, the PtμE/$MoS_2$/Au micro-biosensor shows a linear detection toward miRNA-122 ranging from $10^{-11}$ to $10^{-8}$ M ($S$ = 6.9 nA dec$^{-1}$, $R^2$ = 0.9997), and the detection limit is 1.6 × $10^{-12}$ M ($3\sigma/b$). The PtμE/$MoS_2$/Au micro-biosensor demonstrates good selectivity against other types of proteins and small molecules, and has good reproducibility. Moreover, the PtμE/$MoS_2$/Au micro-biosensor was successfully applied for the measurement of miRNA-122 in real blood samples. Herein, the proposed detection assay could be a potential tool in HCC clinical diagnostics with high sensitivity.

Received 5th June 2023
Accepted 12th July 2023

DOI: 10.1039/d3ra03759b

rsc.li/rsc-advances



## 1. Introduction

Cancer has always been one of the major public health problems worldwide.[1,2] As one of the deadliest cancers both in men and women, hepatocellular carcinoma (HCC), seriously threatens human lives and health with high morbidity and mortality.[1] Accurate and early-stage diagnosis of HCC is vitally important for guiding the treatment and the clinical curative effect, which can significantly improve outcomes and survival.[2,3] Tumor markers are important indicators of the states of cancer. Hence, the detection of tumor markers is extremely important for the diagnosis of its related cancers at an early stage.[4,5] Moreover, the detection of tumor markers with high sensitivity and specificity is always in urgent clinical demand, which is crucially important for the diagnosis of cancer at an early stage and guiding the clinical treatment.[6]

microRNAs (miRNAs), which are only 18–23 nucleotides long in length, play key roles in various cellular functions, and also in tumor progression and metastasis,[7] which makes it to be a new prognostic and therapeutic tool for the management of cancer.[8] Herein, miRNAs could be important biomarkers of stage, progression of cancer.[9] miRNAs have been served as biomarkers for early diagnosis, clinical response and treatment of tumors, and histological classification in the clinical applications.[7] As the most abundant miRNA in the liver, miRNA-122 participates in HCC development and various liver functions.[10] Therefore, the value of miRNA-122 in the blood has been used as the indicator of the HCC for early clinical diagnosis.[11]

Nowadays, the immunoassays have been mainly used in the clinical diagnosis with the merits of high sensitivity and specificity, including electrochemical immunosensor,[12] immunofluorescence,[13] and enzyme-linked immunosorbent assay.[14] However, these detection assays suffer from the problems of expensive antibodies and lengthy preparation, and the biggest drawbacks of standardization and harmonization of theses assays limit their further clinical applications.[6] In addition, the proteomic techniques and molecular biotechniques are also employed for tumor marker analysis.[15,16] However, these methods have the disadvantages of expensive costs, time consuming, and needs skilled operation. Therefore, the development of an innovative sensing assay for the detection of

[a]*School of Rehabilitation Medicine of Binzhou Medical University, Yantai, 264003, China. E-mail: shiyanzhang2007@163.com; gtzhao@bzmc.edu.cn; Fax: +86 535 6913246; Tel: +86 535 6913213*
[b]*Department of Critical Care Medicine, Yantai Yuhuangding Hospital, Yantai, 264003, China*
[c]*The 2nd Medical College of Binzhou Medical University, Yantai, 264003, China*
[d]*Academy of Traditional Chinese and Western Medicine of Binzhou Medical University, Yantai, 264003, China*
[e]*School of Basic Medicine, Binzhou Medical University, Yantai, 264003, China*
† These authors have contributed equally to this work and share first authorship.

miRNA-122 with higher efficiency and easy operation is vital important for HCC diagnosis.

Nowadays, electrochemical sensors have been alternatively used in clinical diagnosis[17] and life sciences[18] with the advantages of low cost, easy operation, flexible substrate, and high sensitivity,[19] especially the electrochemical microsensors based on microelectrode, which have many distinctive merits, such as low currents, steady-state responses, and short response time.[20] Therefore, microelectrodes could be a potential tool for the detection of tumor markers with high accuracy in blood. DNA is one of the most promising biorecognition elements for biosensors toward miRNAs by the hybridization reaction.[21] Therefore, the electrochemical microsensors based on microelectrode combined with probe DNA as biorecognition elements could be attractive alternative strategies for the detection of miRNAs with high sensitivity and efficiency. However, miRNAs detection assays using probe DNA as biorecognition agents through electrochemical microsensors are rather rare.

In this work, a platinum microelectrode was prepared, and modified with molybdenum disulfide ($MoS_2$) and nanocomposite of gold nanoparticle (AuNP), which could not only be used as the solid-contact, but also as the sensing material, especially the AuNP film could be an immobilization matrix for the sulfydryl modified DNA probe. The label-free detection assay was performed through square wave voltammetry (SWV) based on PtμE/$MoS_2$/Au as microsensor for the measurement of miRNA-122 using $[Fe(CN)_6]^{4-/3-}$ as the mediator, and the SWV measurements conditions were optimized to obtain high electrochemical signal.

## 2. Materials and methods

### 2.1 Chemicals

The bovine serum albumin (BSA), PBS (136.89 mM NaCl, 2.67 mM KCl, 8.24 mM $Na_2HPO_4$, 1.76 mM $NaH_2PO_4$, pH 7.2–7.4), and miRNA-122 5′-UGG AGU GUG ACA AUG GUG UUU G-3′, and its sulfydryl modified complement strand of miRNA-122 3′-ACC UCA CAC UGU UAC CAC AAA AAAAAA-SH-5′ were synthesized by Shanghai Sangon Biotech Co., Ltd (Shanghai, China). Human immunoglobulin G (IgG) and DEPC water were purchased from Beyotime Biotechnology. The carcinoembryonic antigen (CEA) protein and alpha fetal protein (AFP) protein were purchased from Fitzgerald Inc. Single layer $MoS_2$ quantum dots were purchased from Nanjing XFNANO Materials Tech Co., Ltd. Monomer 3,4-ethylenedioxythiophene (EDOT, >97%) was purchased from Sigma-Aldrich. Chloroauric acid ($HAuCl_4$) was purchased from Macklin Biotech Co., Ltd (Shanghai, China). The Milli-Q ultrapure water (18.2 MΩ cm-specific resistance) was used throughout. All the other chemicals were of analytical reagent grade.

### 2.2 Fabrication of the platinum microelectrode

A platinum microelectrode, which is denoted as PtμE was fabricated using a platinum wire with a diameter of 21.3 μm (Conghang Co., Ltd, Shanghai, China, 99.9%). The platinum wire was firstly attached to a copper wire by using a conductive silver lacquer. After dried at 60 °C for 6 h, the copper wire attached with platinum wire was carefully inserted into a glass capillary tube with a diameter of 1.5 mm. The copper wire was fixed using non-conducting epoxy glue at the stem end of the capillary tube, and dried at room temperature for 6 h. The platinum wire was flame-fused into the glass from the other tip. The tip of the electrode containing platinum wire was smoothed using a fine grain sandpaper to obtain a platform, other details was followed from the previous work.[22] Then the proposed PtμE electrodes were polished with a 0.05 μm aluminum oxide suspension, and then were chemically cleaned in 1.0 M $HNO_3$ for 15 min followed by ultrasonic cleaning in deionized water and ethanol for 5 min, respectively.

### 2.3 Fabrication of the miRNA-122 micro-biosensors

The $MoS_2$ quantum dots and AuNP were electrodeposited onto the surface of PtμE through two-step galvanostatic electrochemical polymerization. The 0.1 mg $mL^{-1}$ $MoS_2$ quantum dots dispersion containing 0.1 M EDOT was prepared with ultrasonic treatment for ten min, and then used for the first electrodeposition step. The second electrodeposition step was carried out in 1 μM $HAuCl_4$ solution. Each step of the electrodeposition was applied under a constant current of 50 nA for 100 s to produce a total polymerization charge of 5 μC. Moreover, each step of the PtμEs micro-biosensor fabrication was characterized through cyclic voltammetry (CV) in 0.1 M KCl solution using a CHI 660E electrochemical workstation (Shanghai Chenhua Apparatus Corporation, China).

The complement strand of miRNA-122 was used as the probe DNA, and diluted into 10 μM with PBS solution before use. The probe DNA modified with sulfhydryl could be immobilized onto the surface of the PtμE/$MoS_2$/Au electrode after incubation, and the non-specific absorbed probe DNA could be removed through rinsing with PBS buffer. The incubation conditions of the probe DNA with the PtμE/$MoS_2$/Au electrode were optimized to obtain high electrochemical signal, including the concentration of the probe DNA and the incubation time.

### 2.4 Apparatus and measurements

The SWV measurements were performed in the 5.0 mM $[Fe(CN)_6]^{4-/3-}$ solution containing 0.1 M KCl using a CHI 660E electrochemical workstation to characterize the fabrication of the PtμEs/$MoS_2$/Au micro-biosensor. For SWV measurements, the potential range, step potential, amplitude, and frequency were set as from −0.1 to 0.5 V (*vs.* Ag/AgCl, 3 M KCl), 5 mV, 50 mV, and 25 Hz, respectively.[23] The SWV and CV measurements were both carried out through a three-electrode system, in which a PtμEs/$MoS_2$/Au as working electrode, an Ag/AgCl microelectrode with a diameter of 8–10 μm had 3 M KCl as reference electrode, and a Pt wire as counter electrode.

### 2.5. Analytical application

The blood samples were collected from the abdominal aorta of the rats after the rats were sacrificed, and then used for the demonstration of the applicability of the prepared PtμE/$MoS_2$/

Au micro-biosensors for the detection of miRNA-122. The fabricated PtμE/$MoS_2$/Au micro-biosensors were dipped into 20 μL of undiluted blood samples containing various concentrations of miRNA-122 in a 200 μL centrifuge tube. After incubated for 30 min at room temperature, the electrodes were rinsed thoroughly with PBS solution to remove any interference substances. The ion-barrier effect caused by the hybridization between miRNA-122 and the probe DNA blocked the diffusion of $[Fe(CN)_6]^{4-/3-}$ towards the electrode surface, which would lead to a decrease of the electrochemical signal. Therefore, the concentration dependent decrease in the electrical signals could be used for the quantitative measurement of miRNA-122.[24,25]

## 3. Results and discussion

The fabrication scheme of miRNA-122 micro-biosensor is indicated in Scheme 1. The probe DNA modified with sulfhydryl could be attached onto the surface of the PtμE/$MoS_2$/Au through the self-assembly chemistry of Au–S bond, which could lead to the decrease of the peak current of the SWV caused by the reduction of the active area. In addition, the capture of the miRNA-122 through the hybridization with specificity would lead to further decrease of the SWV peak current caused by the ion barrier effect.[24] The net SWV peak current change ($\Delta I$) between the PtμE/$MoS_2$/Au micro-biosensor recorded at *ca.* 0.23 V before and after the incubation with miRNA-122 is used for the quantification detection of miRNA-122.

### 3.1 Cyclic voltammogram measurements

The scanning electron microscope (SEM) was used for the characterization of the morphology of $MoS_2$ and AuNP on the PtμE by the two-step electrodeposition method. As shown in Fig. 1A, thousands of $MoS_2$ nanoparticles with a radius less than 2 nm were considered on the surface of the electrode after first electrodeposition, and AuNP with a radius less than 2 nm can be seen after second electrodeposition (Fig. 1B).[26] The CV scans were also carried out to investigate the electrochemical behaviors of the electrodes after each electrodeposition step. The voltammetric characteristic of the electrode shows a capacitive process with a near-rectangular shape from 0 to 0.5 V in Fig. 2 after each modification,[27] which indicates a high reversibility of the $MoS_2$ and AuNP film.[28] Moreover, the capacitive current of the PtμE/$MoS_2$ at 0.25 V is much higher than the bare electrode, which indicates that the redox capacitance of the electrode is enhanced due to the presence of $MoS_2$ film. The capacitive current of the PtμE/$MoS_2$/Au is more than two times higher than the PtμE/$MoS_2$, therefore the redox capacitance of the electrode is further enhanced after the second modification of the AuNP film. This phenomenon agrees well with the conventional glassy carbon electrode.[29] Moreover, the CV measurements also confirm that the $MoS_2$ and AuNP are successfully electrodeposited onto the PtμE electrodes.

### 3.2 Optimization of the experimental conditions

The SWV measurements were carried out to investigate several experimental conditions which might have influence on the electrochemical performance of the PtμE microsensor toward miRNA-122. As shown in Fig. 3, the SWV response of the PtμE/$MoS_2$/Au microsensor was recorded after the incubation with various concentration of the probe DNA ranging from $10^{-9}$ M to $10^{-6}$ M. The SWV peak current increases with the decrease of the probe DNA concentration (Fig. 3A). The $\Delta I$ between the peak current of the PtμE/$MoS_2$/Au micro-biosensor incubated with various concentrations of the probe DNA was calculated, and the results show that the $\Delta I$ increases with the increase of the probe DNA concentration in the range of $10^{-9}$–$10^{-7}$ M, while when the concentration of the probe DNA is up to $10^{-6}$ M, the $\Delta I$ no more increase, and even shows a slight decrease (Fig. 3B). Hence, $10^{-7}$ M probe DNA is used for further detection assay.

As another important factor affecting the analytical performance, the incubation time of the PtμE/$MoS_2$/Au with probe DNA also needs to be optimized. The optimal incubation time between the probe DNA ($10^{-7}$ M) and PtμE/$MoS_2$/Au electrodes for the formation of PtμE/$MoS_2$/Au micro-biosensor was investigated, and the corresponding SWV response of the PtμE/$MoS_2$/Au electrodes incubated with the probe DNA ($10^{-7}$ M) for different time was recorded (Fig. 4A).

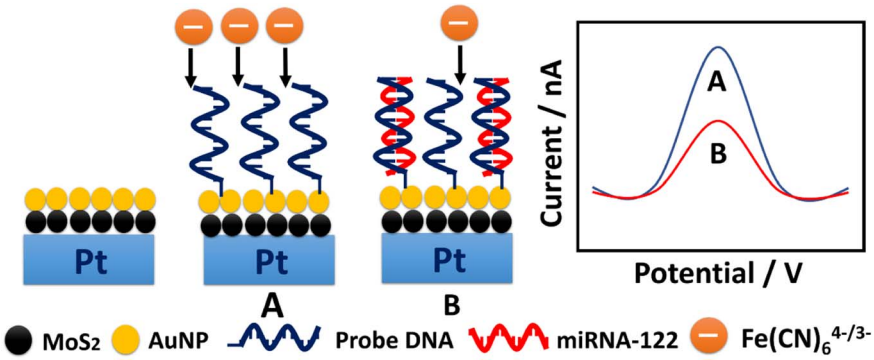


Scheme 1 Schematic illustration of the detection assay toward miRNA-122 through square wave voltammetry in blood based on PtμE/$MoS_2$/Au micro-biosensor using the probe DNA as biorecognition element.

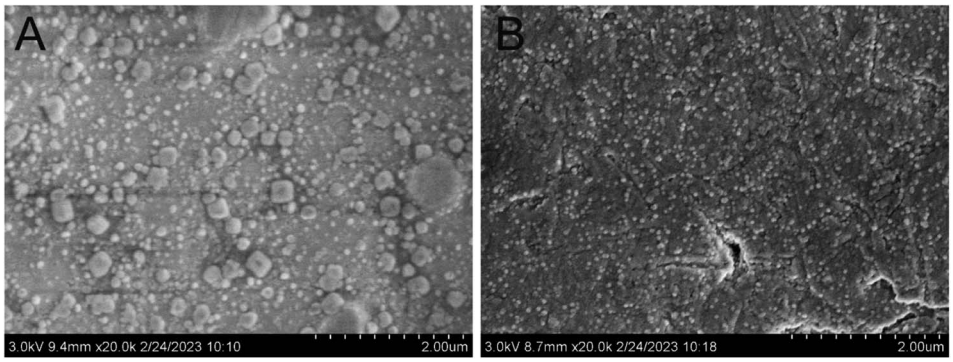


Fig. 1 SEM image of the surface of the PtμE/$MoS_2$ (A) and PtμE/$MoS_2$/Au (B).

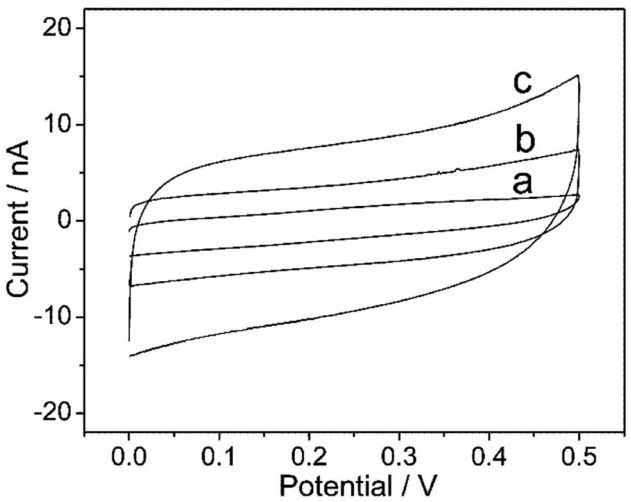


Fig. 2 Cyclic voltammograms of the PtμE electrodes (a) PtμE, (b) PtμE/$MoS_2$, and (c) PtμE/$MoS_2$/Au. The scan rate was 50 mV $s^{-1}$.

The $\Delta I$ between the SWV peak current of the PtμE/$MoS_2$/Au electrodes incubated with the probe DNA for 0 to 1 h was calculated, and as shown in Fig. 4B, $\Delta I$ increases with the increase of the incubation time from 15 min to 0.5 h. While, $\Delta I$ no longer increase when the incubation time is up to 1 h, and even a little decrease instead. Therefore, the incubation time of 0.5 h is selected for further assay.

### 3.3 Sensitivity, selectivity, and reproducibility of the PtμE/$MoS_2$/Au micro-biosensors

The sensitivity of the proposed PtμE/$MoS_2$/Au micro-biosensors under the optimized conditions was assessed, and the effect of miRNA-122 concentration was determined by SWV measurement starting with a concentration of $10^{-8}$ M, and the solution was diluted with DEPC water by *a* factor of 10 until a limit of detection (LOD) could be determined.[23] As expected, the SWV peak current decreases with the increase of the miRNA-122 concentration (Fig. 5A), which is caused by the decrease of the electron transfer efficiency of the $Fe(CN)_6^{4-/3-}$ from the electrolyte to the electrode resulted from the capture of the miRNA-122 by the probe DNA.[12] As shown in Fig. 5B, the calibration plots displayed a good linear relationship of $\Delta I$ between the peak current of the PtμE/$MoS_2$/Au micro-biosensors before and after the incubation with miRNA-122 *versus* various concentration of $10^{-11}$–$10^{-8}$ M ($S$ = 6.9 nA $dec^{-1}$, $R^2$ = 0.9997), and the LOD is 1.6 × $10^{-12}$ M ($3\sigma/b$), where $\sigma$ is the standard deviation of "$n$", which is the number of SWV in blank solution, and $b$ is the slope of the calibration plot (Fig. 5B).[30,31] Obviously, the detection assay developed in this work has good linear range and high sensitivity, and could be used for detection of miRNA-122.

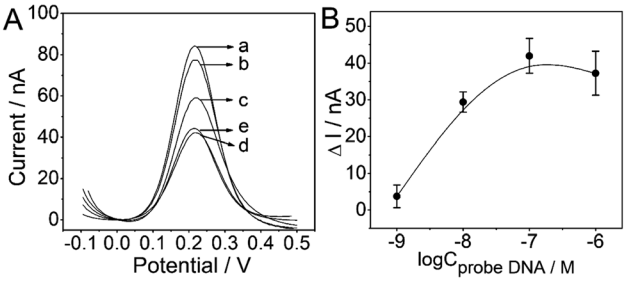


Fig. 3 Electrochemical signal and calibration plot of the PtμE/$MoS_2$/Au miro-biosensors: (A) SWV curve of the PtμE/$MoS_2$/Au electrodes incubated with the probe DNA (a) 0 M, (b) $10^{-9}$ M, (c) $10^{-8}$ M, (d) $10^{-7}$ M, (e) $10^{-6}$ M; (B) SWV calibration plot of PtμE/$MoS_2$/Au electrodes incubated with probe DNA range from $10^{-9}$ M to $10^{-6}$ M.

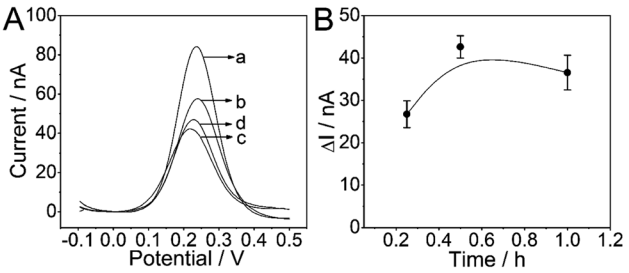


Fig. 4 Electrochemical signal and calibration plot of the PtμE/$MoS_2$/Au miro-biosensors: (A) SWV curve of the PtμE/$MoS_2$/Au electrodes incubated with $10^{-7}$ M probe DNA for (a) 0 M, (b) 0.25 h, (c) 0.5 h, and (d) 1 h; (B) SWV calibration plot of PtμE/$MoS_2$/Au electrodes incubated with $10^{-7}$ M probe DNA for different time range from 0.25 h to 1 h.

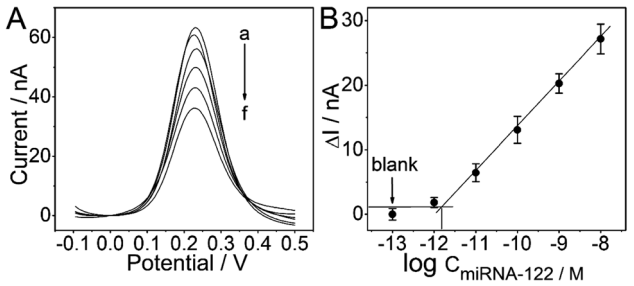


Fig. 5 Electrochemical signal and calibration plot of the PtμE/$MoS_2$/Au miro-biosensors: (A) SWV curve of the PtμE/$MoS_2$/Au micro-biosensors for miRNA-122 (a) blank (b) $10^{-12}$ M, (c) $10^{-11}$ M, (d) $10^{-10}$ M, (e) $10^{-9}$ M, and (f) $10^{-8}$ M; (B) SWV calibration plot of PtμE/$MoS_2$/Au micro-biosensors recorded for miRNA-122 range from $10^{-12}$ M to $10^{-8}$ M.

The specificity of the proposed PtμE/$MoS_2$/Au micro-biosensors against other interfering substances should be also investigated.[32] As shown in Fig. 6, the $\Delta I$ value of the PtμE/$MoS_2$/Au micro-biosensors *versus* $10^{-8}$ M miRNA-122 is much higher than many other interfering proteins in the blood, including CEA, AFP, BSA, and human IgG. Moreover, the PtμE/$MoS_2$/Au micro-biosensors show high selectivity against many small molecules existing in the Hank's solution containing glucose (0.34 g $mL^{-1}$), $K^+$ (0.4 g $mL^{-1}$), $Ca^{2+}$ (0.14 g $mL^{-1}$), and $Na^+$ (8.36 g $mL^{-1}$), which is almost the same with electrolyte of human body. Therefore, the PtμE/$MoS_2$/Au micro-biosensors have good selectivity. The reproducibility of the proposed PtμE/$MoS_2$/Au micro-biosensors is one important factor, and should be determined.[25] Five freshly prepared PtμE/$MoS_2$/Au micro-biosensors were used for miRNA-122 SWV measurements at the concentration of $10^{-8}$ M, and standard deviation is 6.6%. Further, the PtμE/$MoS_2$/Au micro-biosensors can retain 100% of its initial response for five weeks at a storage period of 4 °C, and the initial response can maintain 92.7% even after six weeks storage. Herein, the initial response of the PtμE/$MoS_2$/Au micro-biosensors exhibits a good reproducibility and long-time stability.

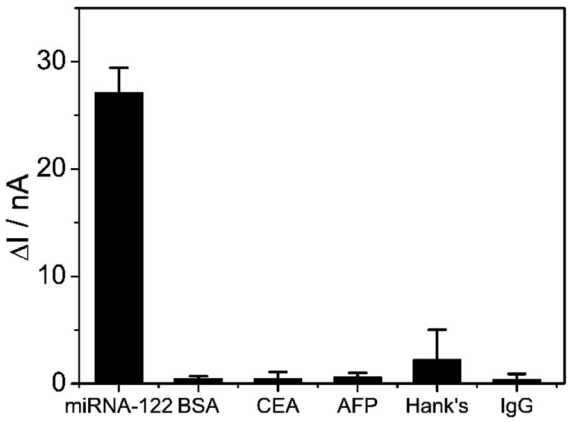


Fig. 6 SWV calibration plot of PtμE/$MoS_2$/Au micro-biosensors recorded for $10^{-8}$ M miRNA-122, 1 μg $mL^{-1}$ AFP, 1 μg $mL^{-1}$ CEA, 1 μg $mL^{-1}$ BSA, 1 μg $mL^{-1}$ human IgG, Hank's solution.

Table 1 Validation of the developed assay ($n = 3$)

| Samples | Added conc. (nM) | Found conc. (nM) | Recovery (%) | RSD (%) |
|---|---|---|---|---|
| Sample 1 | 1 | 1.13 ± 0.34 | 117 | 19.5 |
| Sample 2 | 10 | 11.4 ± 2.48 | 114 | 18.4 |
| Sample 3 | 50 | 48.9 ± 9.78 | 97.8 | 16.8 |

### 3.4 Real sample analysis

The designed detection assay was used for the measurement of miRNA-122 in the real blood to investigate the feasibility of the prepared PtμE/$MoS_2$/Au micro-biosensors in sample analysis. The accuracy and precision of the proposed assay was verified through the standard addition method. As shown in Table 1, the measured recoveries of the proposed assay for miRNA-122 in blood is 97.8–117%, with the RSD values lower than 19.8%, which indicates that the PtμE/$MoS_2$/Au micro-biosensors are available for miRNA-122 analysis in the real blood samples, and has a promising potential for clinical diagnosis with high efficiency and sensitivity.

## 4. Conclusions

In this work, a high efficiency and accuracy detection assay toward miRNA-122 based on PtμE/$MoS_2$/Au micro-biosensors through SWV has been developed. The PtμE/$MoS_2$/Au micro-biosensor was fabricated using PtμE modified with $MoS_2$ and AuNP through two-step electrodeposition as microsensor, and the probe DNA conjugated onto the surface of the PtμE/$MoS_2$/Au is used as the biorecognition element. The proposed detection assay has high sensitivity and feasibility for the detection of miRNA-122 in undiluted blood samples of limited volumes of 20 μL. The proposed detection assay could meet the demand for clinical applications of HCC diagnosis clinically in the future with good selectivity, high efficiency, and reproducibility.

## Author contributions

Jiali Zhai: data curation, writing – original draft. Huiyuan Sun: data curation, writing – original draft. Mingkang Li: data curation. Yuhao Gao: data curation. Zhi Gao: data curation. Xiyu Xie: data curation. Yixin Hu: data curation. Lixia Zhang: formal analysis. Guangtao Zhao: writing – review & editing.

## Conflicts of interest

There are no conflicts to declare.

## Acknowledgements

This work was supported by the Natural Science Foundation of Shandong Province (ZR2020MC076).

## References

1 R. L. Siegel, K. D. Miller, H. E. Fuchs and A. Jemal, Cancer statistics, 2022, *Ca-Cancer J. Clin.*, 2022, **72**, 7–33.
2 H. Zhao, M. Wang, X. Xiong, Y. Liu and X. Chen, Simultaneous fluorescent detection of multiplexed miRNA of liver cancer based on DNA tetrahedron nanotags, *Talanta*, 2020, **210**, 1–7.
3 T. Gao, J. Zhi, C. Mu, S. Gu, J. Xiao, J. Yang, Z. Wang and Y. Xiang, One-step detection for two serological biomarker species to improve the diagnostic accuracy of hepatocellular carcinoma, *Talanta*, 2018, **178**, 89–93.
4 H. Tang, H. Wang, C. Yang, D. Zhao, Y. Qian and Y. Li, A novel strategy for nanopore-based selective detection of single carcinoembryonic antigen (CEA) molecules, *Anal. Chem.*, 2020, **4**, 3042–3049.
5 X. Gao, S. Niu, J. Ge, Q. Luan and G. Jie, 3D DNA nanosphere-based photoelectrochemical biosensor combined with multiple enzyme-free amplification for ultrasensitive detection of cancer biomarkers, *Biosens. Bioelectron.*, 2020, **147**, 1–8.
6 L. Qi, S. Liu, Y. Jiang, J. Lin, L. Yu and Q. Hu, Simultaneous detection of multiple tumor markers in blood by functional liquid crystal sensors assisted with target-induced dissociation of aptamer, *Anal. Chem.*, 2020, **5**, 3867–3873.
7 L. Wu, W. B. Zhou, J. Zhou, Y. Wei, H. M. Wang, X. D. Liu, X. C. Chen, W. Wang, L. Ye, L. C. Yao, Q. H. Chen and Z. G. Tang, Circulating exosomal microRNAs as novel potential detection biomarkers in pancreatic cancer, *Oncol. Lett.*, 2020, **2**, 1432–1440.
8 N. Chauhan, A. Dhasmana, M. Jaggi, S. C. Chauhan and M. M. Yallapu, miR-205: A potential biomedicine for cancer therapy, *Cells*, 2020, **9**, 1–29.
9 W. Chen, J. Song, H. Bian, X. Yang, X. Xie, Q. Zhu, C. Qin and J. Qi, The functions and targets of miR-212 as a potential biomarker of cancer diagnosis and therapy, *J. Cell. Mol. Med.*, 2020, **4**, 2392–2401.
10 F. Chen, F. Zhang, Y. Liu and C. Q. Cai, Simply and sensitively simultaneous detection hepatocellular carcinoma markers AFP and miRNA-122 by a label-free resonance light scattering sensor, *Talanta*, 2018, **186**, 473–480.
11 M. Dai, L. Li and X. Qin, Clinical value of miRNA-122 in the diagnosis and prognosis of various types of cancer, *Onol. Lett.*, 2019, **4**, 3919–3929.
12 X. Chen, X. Jia, J. Han, J. Ma and Z. Ma, Electrochemical immunosensor for simultaneous detection of multiplex cancer biomarkers based on graphene nanocomposites, *Biosens. Bioelectron.*, 2013, **50**, 356–361.
13 H. Li, Z. Cao, Y. Zhang, C. Lau and J. Lu, Simultaneous detection of two lung cancer biomarkers using dual-color fluorescence quantum dots, *Analyst*, 2011, **7**, 1399–1405.
14 Y. Yen, C. Chao and Y. Yeh, A graphene-PEDOT:PSS modified paper-based aptasensor for electrochemical impedance spectroscopy detection of tumor marker, *Sensors*, 2020, **5**, 1–11.
15 V. C. Hodgkinson, V. Agarwal, D. ELFadl, J. N. Fox, P. L. McManus, T. K. Mahapatra, P. J. Kneeshaw, P. J. Drew, M. J. Lind and L. Cawkwell, Pilot and feasibility study: comparative proteomic analysis by 2-DE MALDI TOF/TOF MS reveals 14-3-3 proteins as putative biomarkers of response to neoadjuvant chemotherapy in ER-positive breast cancer, *J. Proteomics*, 2012, **9**, 2745–2752.
16 H. Koike, D. Ichikawa, H. Ikoma, E. Otsuji, K. Kitamura and H. Yamagishi, Comparison of methylation-specific polymerase chain reaction (MSP) with reverse transcriptase-polymerase chain reaction (RT-PCR) in peripheral blood of gastric cancer patients, *J. Surg. Oncol.*, 2004, **4**, 182–186.
17 A. A. M. Abdurhman, Y. Zhang, G. Zhang and S. Wang, Hierarchical nanostructured noble metal/metal oxide/graphene-coated carbon fiber: in situ electrochemical synthesis and use as microelectrode for real-time molecular detection of cancer cells, *Anal. Bioanal. Chem.*, 2015, **26**, 8129–8136.
18 Y. Chen, C. Guo, L. Lim, S. Cheong, Q. Zhang, K. Tang and J. Reboud, Compact microelectrode array system: tool for in situ monitoring of drug effects on neurotransmitter release from neural cells, *Anal. Chem.*, 2008, **4**, 1133–1140.
19 J. Bobacka, A. Ivaska and A. Lewenstam, Potentiometric ion sensors, *Chem. Rev.*, 2008, **2**, 329–351.
20 R. J. Forster, Microelectrodes: new dimensions in electrochemistry, *Chem. Soc. Rev.*, 1994, **23**, 289–297.
21 Y. H. Roh, R. C. H. Ruiz, S. Peng, J. B. Lee and D. Luo, Advances in DNA-based nanotechnology themed issue, *Chem. Soc. Rev.*, 2011, **40**, 5730–5744.
22 J. L. Zhai, P. Y. Ji, Y. Xin, Y. F. Liu, Q. W. Qu, W. T. Han and G. T. Zhao, Development of carcinoembryonic antigen rapid detection system based on platinum microelectrode, *Front. Chem.*, 2022, **10**, 1–8.
23 S. Hannah, M. Al-Hatmi, L. Gray and D. K. Corrigan, Low-cost, thin-film, mass-manufacturable carbon electrodes for detection of the neurotransmitter dopamine, *Bioelectrochemistry*, 2020, **133**, 1–9.
24 F. Gao, Y. Chu, Y. Ai, W. Yang, Z. Lin and Q. Wang, Hybridization induced ion-barrier effect for the label-free and sensitive electrochemical sensing of Hepatocellular Carcinoma biomarker of miRNA-122, *Chin. Chem. Lett.*, 2021, **7**, 2192–2196.
25 M. Rizwan, S. Elma, S. A. Lim and M. U. Ahmed, AuNPs/CNOs/SWCNTs/chitosan-nanocomposite modified electrochemical sensor for the label-free detection of carcinoembryonic antigen, *Biosens. Bioelectron.*, 2018, **107**, 211–217.
26 M. Vizza, W. Giurlani, L. Cerri, N. Calisi, A. A. Leonardi, M. J. L. Faro, A. Irrera, E. Berretti, J. V. Perales-Rondón, A. Colina, E. Bujedo Saiz and M. Innocenti, Electrodeposition of molybdenum disulfide ($MoS_2$) nanoparticles on monocrystalline silicon, *Molecules*, 2022, **27**, 1–12.
27 G. A. Crespo, S. Macho, J. Bobacka and F. X. Rius, Transduction mechanism of carbon nanotubes in solid-

contact ion-selective electrodes, *Anal. Chem.*, 2009, **2**, 676–681.

28 C. Ocaña, N. Abramova, A. Bratov, T. Lindfors and J. Bobacka, Calcium-selective electrodes based on photo-cured polyurethane-acrylate membranes covalently attached to methacrylate functionalized poly(3,4-ethylenedioxythiophene) as solid-contact, *Talanta*, 2018, **186**, 279–285.

29 T. Yin, D. Pan and W. Qin, A solid-contact $Pb^{2+}$-selective polymeric membrane electrode with Nafion-doped poly(pyrrole) as ion-to-electron transducer, *J. Solid State Electrochem.*, 2012, **2**, 499–504.

30 A. Shah, A. Nisar, K. Khan, J. Nisar, A. Niaz, M. N. Ashiq and M. S. Akhter, Amino acid functionalized glassy carbon electrode for the simultaneous detection of thallium and mercuric ions, *Electrochim. Acta*, 2019, **321**, 1–8.

31 P. Gupta, K. Tsai, C. K. Ruhunage, V. K. Gupta, C. E. Rahm, D. Jiang and N. T. Alvarez, True picomolar neurotransmitter sensor based on open-ended carbon nanotubes, *Anal. Chem.*, 2020, **12**, 8536–8545.

32 Q. Zhai, X. Zhang, Y. Xia, J. Li and E. Wang, Electrochromic sensing platform based on steric hindrance effects for CEA detection, *Analyst*, 2016, **13**, 3985–3988.